Original Article

Protective effects of resveratrol on postmenopausal osteoporosis: regulation of SIRT1-NF-κB signaling pathway

Jing Feng[1], Shuai Liu[1], Sai Ma[2], Jian Zhao[1], Wei Zhang[1], Wei Qi[1], Pengchong Cao[1], Zheng Wang[3]*, and Wei Lei[1]*

[1]Department of Orthopedics, Xijing Hospital, Fourth Military Medical University, Xi'an 710032, China
[2]Department of Cardiology, Xijing Hospital, Fourth Military Medical University, Xi'an 710032, China
[3]Department of Orthopedics, China PLA General Hospital, Beijing 100853, China
*Correspondence address. Tel/Fax: +86-29-84771011; E-mail: leiwei@fmmu.edu.cn (W.L.)/E-mail: Wangzheng301@163.com (Z.W.)

Postmenopausal osteoporosis severely jeopardizes human health. Seeking for therapeutic drugs without side effects is of great necessity. Our study was designed to investigate whether resveratrol, an agonist of SIRT1, could have favorable effect on osteoporosis and to explore the underlying mechanisms. Rat osteoporosis model (ovariectomy group, OVX) was established by bilateral ovariectomy. Three different doses of resveratrol were used: 5 mg/kg/d (low-dosed, RES^LD), 25 mg/kg/d (medium-dosed, RES^MD), and 45 mg/kg/d (high-dosed, RES^HD). Results showed that RES^LD did not show any significant effect on OVX alterations, while RES^MD and RES^HD significantly elevated the decreased bone mineral density induced by osteoporosis (RES^MD 0.205 ± 0.023, RES^HD 0.214 ± 0.053 vs. OVX 0.165 ± 0.050 g/cm^2 respectively; $P < 0.05$). Serum markers alkaline phosphatase (ALP) and osteocalcin were moderately restored by resveratrol. Moreover, resveratrol improved bone structure in OVX rats, demonstrated by hematoxylin-eosin staining and micro-computed tomographic results. *In vitro* results revealed that resveratrol promoted osteoblast differentiation of bone marrow mesenchymal stromal cells, evidenced by the increase of ALP generation and mRNA expression of collagen 1 ($P < 0.05$; RES^MD, RES^HD vs. control group). *SIRT1* gene silencing by siRNA transfection blocked these beneficial effects of resveratrol ($P < 0.05$; RES + SIRT1^KD vs. RES^HD). Western blot results showed that resveratrol activated SIRT1 and subsequently suppressed the activity of NF-κB with decreased expression level of p-IκBα and NF-κB p65 ($P < 0.05$). Our findings verified the effects of specific dosed resveratrol on postmenopausal osteoporosis through osteoblast differentiation via SIRT1-NF-κB signaling pathway. This study suggested the therapeutic potential of resveratrol against osteoporosis and stressed the importance of effective doses.

Keywords   resveratrol; osteoporosis; sirtuin 1

Introduction

Postmenopausal osteoporosis, characterized by low bone mineral density (BMD) and microarchitectural deterioration of bone tissue, is a major concern for public health [1]. Decrease of BMD in osteoporosis increases the risk of bone fractures [2]. Consequent osteoporotic fractures impact negatively on quality of life and increase the morbidity and mortality in post-menopausal women [3,4].

Estrogen deficiency is a predominant cause for postmenopausal osteoporosis, which contributes to the increase of bone turnover, and subsequently lowering bone mineral content and bone structure destruction [5]. Though estrogen replacement therapies have shown therapeutic effects on osteoporosis treatment, their benefits are compromised by serious side effects, such as increased risk of breast and uterine cancers, as well as high cost [6]. Therefore, seeking for drugs to reverse the tendency of bone loss with the least side effect is of great necessity. Recently, metabolism-related drugs have emerged as potential drugs for osteoporosis because of their bone formation effects.

Sirtuins (SIRT1–7), a class of NAD$^+$-dependent deacetylases, could exert beneficial effects in many diseases due to their critical role in metabolism [7]. SIRT1 is the most widely studied molecule in sirtuin family. The activation of SIRT1 could affect various physiological and pathological processes, such as cell proliferation and differentiation, inflammation, anti-oxidative response, and osteoporosis process [8,9]. Resveratrol, a specific agonist of SIRT1, has been shown to play a positive role in neural, cardiovascular, and orthopedic diseases [10]. Furthermore, several studies reported the potential therapeutic role of resveratrol in osteoporosis, whereas the specific dose of resveratrol was inclusive. Previous reports found that resveratrol could exert osteogenic effects *in vitro*, which may further alleviate the

extent of osteoporosis [11–13]. Moreover, the underlying mechanisms of resveratrol on osteoporosis are unclear and the dose of resveratrol in osteoporotic model *in vivo* is still controversial. Therefore, we aimed to combine both *in vivo* and *in vitro* studies to explore the protective effects of resveratrol and to find out the downstream molecules.

Our present study was designed to investigate the protective role of resveratrol on osteoporosis both *in vivo* and *in vitro*, and more importantly, to explore the underlying molecular mechanisms.

Materials and Methods

Rat model of postmenopausal osteoporosis
All animal procedures were conducted according to the protocols approved by the Institutional Animal Care and Use Committee of Xijing Hospital, Fourth Military Medical University. All animal experiments were performed in accordance with the National Institutes of Health Guidelines for the Use of Laboratory Animals. Female Sprague-Dawley (SD) rats (3-month old, weighing 280–350 g) were purchased from the Animal Center of Fourth Military Medical University. Animals were kept at 26–28°C with free access to water and chow. Rats were randomized into the following groups: control group (Con) ($n = 8$), ovariectomy group (OVX) ($n = 8$), and ovariectomy + resveratrol group (RES) ($n = 24$). RES group was further divided into three groups: low-dose group (RES^{LD}), middle-dose group (RES^{MD}), and high-dose group (RES^{HD}). Bilateral ovariectomy was conducted under anesthesia by persistent 2% isoflurane inhalation after laparotomy. The criteria for successful anesthesia were regularly respiratory rhythm and absence of retraction reflex in hind-legs after mechanical stimulation. In the control group, rats underwent laparotomy without ovariectomy. Rats were injected with penicillin for three consecutive days after operation to prevent infection. In RES group, resveratrol (Sigma, St Louis, USA) was orally administrated at the dosage of 5, 25, and 45 mg/kg/d (RES^{LD} group, RES^{MD} group, and RES^{HD} group), respectively, 7 days after operation for 8 weeks.

Isolation and culture of bone marrow mesenchymal stromal cells
In the *in vitro* study, rats were divided into control, RES^{LD}, RES^{MD}, RES^{HD}, and RES + SIRT1^{KD} groups. Bone marrow tissues of SD rats (2–3 weeks old) were washed with phosphate buffered saline (PBS) containing 1% antibiotic/antimycin to prevent bacterial contamination. The suspension was collected, centrifuged at 200 g for 10 min and put into the cell culture flask. The cells were maintained in Dulbecco's modified Eagle's medium/F-12 (DMEM/F-12; Hyclone, Logan, USA) with 10% (v/v) fetal bovine serum (FBS; Hyclone) for 72 h at 37°C with 5% CO_2. Adherent

cells were digested and transferred into a new cell culture flask. Bone marrow mesenchymal stromal cells (BMSCs) were cultured with DMEM/F-12/10% FBS with 2 ng/ml basic fibroblast growth factor (Peprotech, Rocky Hill, USA) and 1% antibiotic/antimycin. The medium was refreshed every two days. Then a trypsin solution (0.05% trypsin + 0.02% ethylenediaminetetraacetic acid; Invitrogen, Carlsbad, USA) was used for cell passages. Resveratrol was dissolved with DMSO at the concentration of 100 mM. After cell attachment, in resveratrol treated groups (RES^{LD}, RES^{MD}, and RES^{HD}), cells were subject to 24 h of resveratrol treatment at final concentrations of 20, 25, and 30 μM, respectively; while in control group, cells were treated with same-volume DMSO. To silence SIRT1 gene expression, small interfering RNA (siRNA) of SIRT1 was synthesized as the following sequences according to published article: sense strand 5′-GCGAUGUUAUAAUUAAUGAtt-3′ and the antisense strand 5′-UCAUUAAUUAUAACAUCGCag-3′ [14]. The knockdown efficiency of siRNA was preliminarily analyzed by real-time polymerase chain reaction (PCR) and western blot analysis (**Supplementary Fig. S1**). Lipofectamine 2000 (Invitrogen) was added during siRNA transfection. In RES+ SIRT1^{KD} group, after cell attachment, cells were continuously cultured with the medium containing resveratrol at the concentration of 30 μM. Additionally, 100 nM siRNA was added to the medium and cells were incubated with siRNA for 48 h and then collected.

Bone mineral density measurement
BMD was measured with dual-emission X-ray absorptiometry (DEXA) method using a dual energy X-ray absorptiometry (Lunar, Madison, USA) and relevant assessment software. Vertebra of lumbar spine (L3) and right femur bone of each rat were placed in the imaging positioning tray and scanned. All specimens were placed in a similar orientation. BMD was evaluated by inclusion of the whole specimen in the region of interest. The measurement was performed in a blind manner.

Histological staining
The left femoral condyle of each rat was obtained and fixed in 4% paraformaldehyde for 24 h and then decalcified for 2 weeks in 10% EDTA buffer (pH 7.0). The samples were dehydrated, embedded in paraffin and cut into slices (about 4 μm thick). Slices were stained with hematoxylin-eosin (HE). The sections were visualized by using an optical microscope (Leica, Wetzlar, Germany) and photographed.

Micro-computed tomography
Micro-computed tomography (CT) technique was used to evaluate bone structural and mineral changes in rats. Briefly, vertebras of lumbar spine (L4) were isolated from rats after sacrifice. Muscles and ligaments were carefully excised. Then the vertebral specimens ($n = 8$) from each group were

placed in a similar orientation and micro-CT scanned (eXplore Locus SP micro-CT; GE Healthcare, Wisconsin, USA). The X-ray source voltage was set at 80 kV and beam current at 200 mA using filtered Bremsstrahlung radiation. To determine the 3D micro-architectural properties, specimens were evaluated with analysis software (Microview; GE Healthcare). All scans and calculations were performed by the same investigator in the blind manner.

ELISA assay
At the end of the experimental period, the blood sample (2 ml) was collected from the right common carotid artery and placed into Eppendorf tubes. Samples were placed at room temperature for 4 h, followed by a centrifugation for 20 min (3000 g at 4°C). Aliquots of the supernatant were removed and stored at −80°C before assay. According to the manufacturer's instruction, serum levels of alkaline phosphatase (ALP) and osteocalcin (OC) were measured by colorimetric analysis using a spectrophotometer at a wavelength of 450 nm with the detection kit (BIKW, Beijing, China).

Western blot assay
Samples were extracted from cultured BMSCs. For whole cell extracts, the collected cells were then lysed in an ice-cold RIPA buffer containing 1% protease inhibitor cocktail (Sigma). The sample was centrifuged at 12,000 g for 20 min at 4°C. The supernatant was collected, aliquoted and stored at −80°C. For nuclear extracts of BMSCs, cells were trypsinized and washed twice with cold PBS. Cells were resuspended in hypotonic lysis buffer containing protease inhibitor for 15 min. A total of 12.5 μl of 10% Nonidet P-40 was added and mixed for 15 s. The extracts were centrifuged for 1.5 min. The supernatants (cytoplasmic extracts) were removed. About 25 μl of ice-cold nuclear extraction buffer was added to the pellets and incubated for 30 min. Extracts were centrifuged, and the supernatant (nuclear extracts) was stored at −80°C. The protein concentration was measured by the modified Bradford assay (Bio-Rad, Hercules, USA), then the proteins were separated by sodium dodecyl sulfate-polyacrylamide gel electrophoresis, transferred to nitrocellulose membranes and probed with primary antibodies against SIRT1 (dilution 1 : 8000; Abcam, Cambridge, USA); p-IκBα (dilution 1 : 1000; Bioworld, Beijing, China); NF-κB p65 (dilution 1 : 1000; Santa Cruz, Santa Cruz, USA) or histone H3 (dilution 1 : 1000; Abcam) overnight at 4°C followed by the incubation with the corresponding horseradish peroxidase-conjugated secondary antibodies at room temperature for 1 h. The signal was detected using an enhanced chemiluminescence reagent kit (Millipore, Billerica, USA). The western blot bands were visualized with UVP Bio-Imaging Systems (UVP, Upland, USA). The densities

were analyzed with Vision Works LS Acquisition and Analysis Software (UVP).

In vitro differentiation of osteoblasts
In vitro osteoblastogenesis was carried out using BMSCs. To induce osteoblast differentiation, cells were cultured by medium supplemented with 50 mg/l L-ascorbic acid, 10 nM dexamethasone and 10 mM Na⁺-glycerophosphate. ALP staining was performed on culture day 14 and ALP activity was measured according to standard protocols.

Real-time PCR
Total RNA was isolated from BMSCs. The cDNA was synthesized using the commercial RT-PCR kit (PrimeScript® RT Master Mix Perfect Real Time; TaKaRa, Dalian, China). Real-time PCR was performed using the real-time PCR commercial kit (SYBR® Premix Ex Taq™ II; TaKaRa). Data were normalized to house-keeping gene _GAPDH_. Primers were designed according to the sequence in previous report [15] and synthesized by TaKaRa. The primer sequences are shown as the follows: _SIRT1_ forward 5′-ACAACCTCCTGTT GGCTGATG-3′ and reverse 5′-GCTTGCGTGTGATGCT CTGT-3′; _collagen 1_ forward 5′-TCTCCACTCTTCTAGTT CCT-3′ and reverse 5′-TTGGGTCATTTCCACATGC-3′; _osteopontin_ forward 5′-CTACAGTCGATGTCCCCAAC-3′ and reverse 5′-GACTCCTTAGACTCACCGCT-3′; and _GAPDH_ forward 5′-GGCACAGTCAAGGCTGAGAATG-3′ and reverse 5′-ATGTGGTGAAGACGCCAGTA-3′.

Statistical analysis
All statistical analyses were performed by SPSS software (version 15.0; SPSS Inc., Chicago, USA). All data are expressed as the mean ± standard deviation. Statistical differences between different groups were analyzed using one-way analysis of variance and Newman–Keuls post test. Statistical significance was set at $P < 0.05$.

Results

Resveratrol treatment restored BMD in ovariectomized rat
As shown in **Table 1** and **Fig. 1**, there was no statistically significant difference among groups at base line. In OVX group, BMD was significantly decreased compared with control group (0.165 ± 0.050 vs. 0.249 ± 0.029 g/cm²; $P < 0.05$). BMD was moderately elevated in RES^LD group compared with OVX group (0.173 ± 0.041 vs. 0.165 ± 0.050 g/cm²; $P > 0.05$). And this elevation was of statistical significance in RES^MD and RES^HD groups (RES^MD: 0.205 ± 0.023 vs. 0.165 ± 0.050; RES^HD: 0.214 ± 0.053 vs. 0.165 ± 0.050 g/cm²; $P < 0.05$).

The levels of ALP and OC were increased in ovariectomized rat

ELISA assay was performed to measure serum biochemical markers ALP and OC. Results were summarized in **Table 2** and **Fig. 1**. Both ALP and OC were increased in OVX group compared with control group (ALP: 237.1 ± 39.2 vs. 122.5 ± 31.1 U/l; OC: 49.7 ± 9.1 vs. 23.7 ± 8.5 ng/cm; $P < 0.05$). Both ALP and OC were moderately decreased after low, medium, and high dose of resveratrol treatment compared with OVX group (for ALP, RES^{LD}: 194.3 ± 42.60, RES^{MD}: 171.8 ± 47.44, RES^{HD}: 160.8 ± 39.63 U/l; $P > 0.05$; for OC, RES^{LD}: 45.00 ± 10.80, RES^{MD}: 40.50 ± 16.36, RES^{HD}: 37.00 ± 10.98 ng/cm; $P > 0.05$), but this decrease was of no significant difference.

Resveratrol treatment improved morphological changes in osteoporosis rat model

Osteoporotic changes in the bones of osteoporotic rats were histologically confirmed by HE staining (**Fig. 2**). Thinning of bone trabeculae, and increase of intertrabecular space and microfractures of bone trabeculae (judged by the generation of connective tissue in the border zone of fractured trabeculae) were observed in OVX rats. In the section of the rats receiving resveratrol administration, improved bone trabeculae and intertrabecular space and fewer microfractures of bone

Table 1. Effects of resveratrol administration on BMD (g/cm^2)

Group	Baseline	After the experiment
Control	0.245 ± 0.038	0.249 ± 0.029
OVX	0.243 ± 0.031	$0.165 \pm 0.050^{\#}$
RES^{LD}	0.242 ± 0.043	0.173 ± 0.041
RES^{MD}	0.241 ± 0.029	$0.205 \pm 0.023*$
RES^{HD}	0.243 ± 0.052	$0.214 \pm 0.053*$

BMD, bone mineral density.
$^{\#}P < 0.05$ vs. control group; $*P < 0.05$ vs. OVX group.

trabeculae were found. Furthermore, these protective effects against OVX changes were in a dose-dependent manner.

The change of parameters of micro-CT

The indicators of micro-CT include bone volume/total volume (BV/TV), bone surface/bone volume (BS/BV), trabecular thickness (Tb. Th), trabecular number (Tb. N), trabecular separation (Tb. Sp), and BMD. As shown in **Table 3**, in OVX group, BS/BV and Tb. Sp were increased while BV/TV, Tb. Th, Tb. N, and BMD were decreased, indicating the formation of osteoporosis in OVX rats ($P < 0.05$). The increase of BS/BV and Tb. Sp were diminished in RES groups, and the resveratrol treatment significantly restored the reduction of BV/TV, Tb. Th, Tb. N and BMD, suggesting the improvement of osteoporosis. Parameters of micro-CT were significantly improved in medium and high doses resveratrol treatment groups ($P < 0.05$) but not in low dose group. The 3D reconstructed images of vertebras of lumbar spine were shown in **Fig. 3**.

Resveratrol increased osteoblast differentiation and activity *in vitro*

ALP staining and activity analysis were performed to reflect the level of osteoblast differentiation. As shown in **Fig. 4A,B**, ALP staining and activity were significantly increased in RES^{MD} and RES^{HD} groups compared with control group, indicating enhanced osteoblast differentiation (RES^{MD}: 0.2250 ± 0.0420 vs. 0.1175 ± 0.0171; RES^{HD}: 0.2375 ± 0.0479 vs. 0.1175 ± 0.0171 nmol/µg protein/min; $P < 0.05$). While in RES + SIRT1^{KD} group, ALP staining and activity were significantly decreased (0.0700 ± 0.0258 vs. 0.1175 ± 0.0171 nmol/µg protein/min; $P < 0.05$), indicating that the effect of resveratrol was blocked by siRNA-SIRT1.
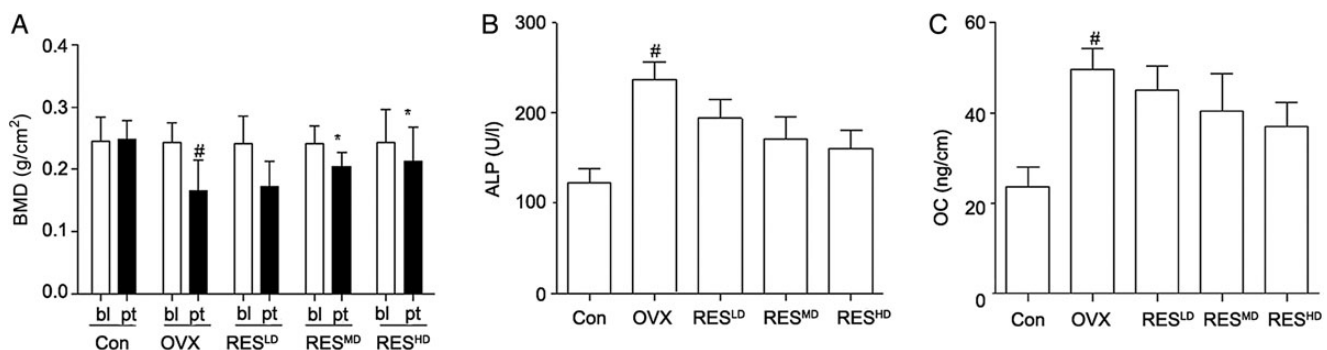
Moreover, real-time PCR analysis revealed that the expression levels of osteoblast-specific genes, such as *type I collagen* and *osteopontin*, were significantly elevated in

Figure 1. Bone mineral density (BMD) and serum bio-marker [alkaline phosphatase (ALP) and osteocalcin (OC)] changes in ovariectomy (OVX) and resveratrol treated groups (A) Resveratrol treatment restored BMD reduction in OVX rats. (B) ALP changes in control, OVX and resveratrol treated groups. (C) OC changes in control, OVX and resveratrol treated groups. $^{\#}P < 0.05$ vs. control group; $*P < 0.05$ vs. OVX group. bl: baseline; pt: post-treatment.

medium and high doses resveratrol treatment groups compared with control group (for *type I collagen*, RES^{MD}: 1.340 ± 0.133; RES^{HD}: 1.405 ± 0.187; $P < 0.05$; for osteopontin, RES^{MD}: 1.293 ± 0.086; RES^{HD}: 1.358 ± 0.103; $P < 0.05$). On the contrary, in RES + SIRT1^{KD} group, *SIRT1* gene silencing by siRNA decreased the mRNA expression of both *type I collagen* and *osteopontin* (for *type I collagen*: 0.6875 ± 0.0943; for *osteopontin*: 0.6650 ± 0.1139; $P < 0.05$), counteracting the beneficial effects of resveratrol. Taken together, these results suggested a positive correlation of osteoblast differentiation with SIRT1 protein expression (**Fig. 4C**). Furthermore, low dose of resveratrol *in vitro* did not cause significant alterations in osteoblast-specific genes expression.

Table 2. Effects of resveratrol treatment on serum bio-markers (ALP and OC)

| Group	ALP (U/l)	OC (ng/ml)
Control	122.5 ± 31.1	23.7 ± 8.5
OVX	237.1 ± 39.2$^{\#}$	49.7 ± 9.1$^{\#}$
RESLD	194.3 ± 42.6	45.5 ± 10.8
RESMD	171.8 ± 47.4	40.5 ± 16.4
RESHD	160.8 ± 39.6	37.1 ± 10.9

$^{\#}P < 0.05$ vs. control group.
ALP, alkaline phosphatase; OC, osteocalcin.

Resveratrol-induced SIRT1 activation and subsequent NF-κB suppression

As revealed by the western blot results (**Fig. 5**), resveratrol treatment significantly elevated the expression of SIRT1 in BMSCs and this beneficial effect was dose dependent ($P < 0.05$). In RES+ SIRT1^{KD} group, SIRT1 knockdown by siRNA interference effectively decreased the elevated protein level of SIRT1 induced by resveratrol. At the same time, the nuclear expression levels of NF-κB p65 and p-IκBα (normalized to reference protein β-actin) were decreased in resveratrol treatment groups compared with control group, indicating suppressed NF-κB activity. On the contrary, NF-κB p65 and p-IκBα were down-regulated after *SIRT1* gene silencing in RES + SIRT1^{KD} group.

Discussion

In this study, we verified that resveratrol treatment with doses of 25 and 45 mg/kg/d could restore osteoporosis-induced BMD reduction and microarchitectural deterioration in ovariectomized rat model. Furthermore, resveratrol treatment promoted osteoblast differentiation and activity of BMSCs. More importantly, it was found that resveratrol-mediated SIRT1 activation inhibited the phosphorylation and activity of NF-κB p-IκBα and NF-κB p65 and siRNA-SIRT1 blocked the beneficial effects of resveratrol, demonstrating that the protective function of resveratrol was via the SIRT1-NF-κB signaling pathway.
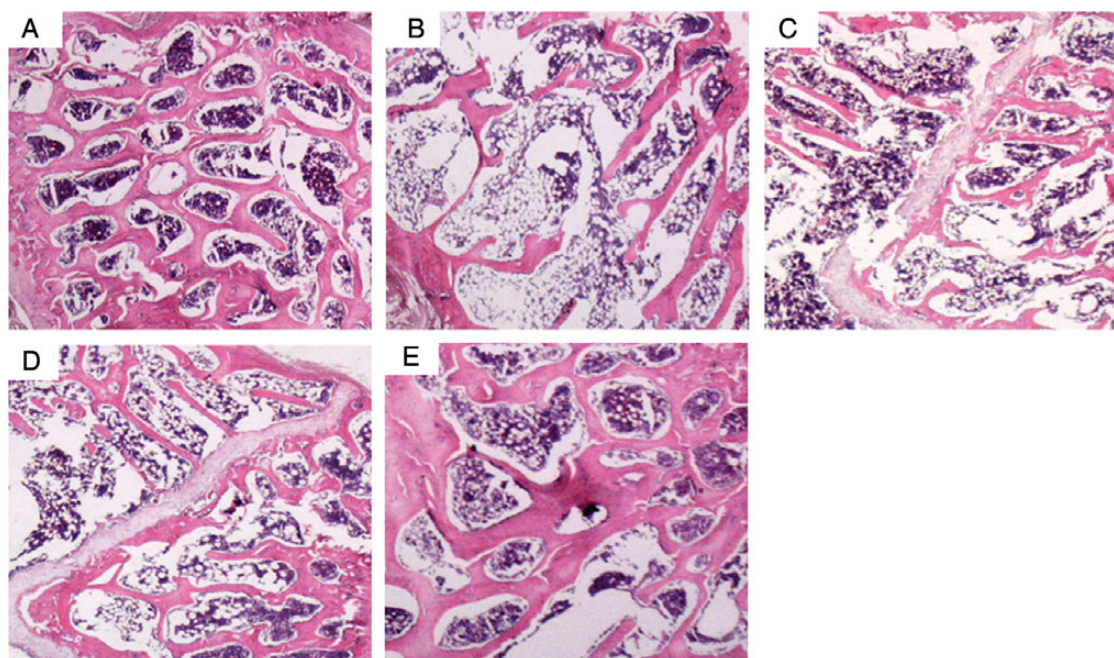
Figure 2. Morphological picture of proximal metaphysis of femoral bone (A) Control rats. (B) The rat after ovariectomy. (C) The rat after ovariectomy treated with low-dose resveratrol. (D) The rat after ovariectomy treated with medium-dose resveratrol. (E) The rat after ovariectomy treated with high-dose resveratrol.

Table 3. Parameters of micro-CT

Group	BMD (mg/cm^3)	BV/TV (%)	BS/BV (1/mm)	Tb.Th (μm)	Tb.N (1/mm)	Tb.Sp (mm)
Control	414 ± 52	45 ± 5	20 ± 4	101 ± 20	4.5 ± 0.5	0.12 ± 0.03[#]
OVX	152 ± 42[#]	10 ± 3[#]	40 ± 5[#]	47 ± 11[#]	1.8 ± 0.6[#]	0.49 ± 0.07[#]
RES[LD]	201 ± 32	15 ± 3	33 ± 5	61 ± 10	2.5 ± 0.5*	0.44 ± 0.04
RES[MD]	330 ± 52*	28 ± 3*	26 ± 3	83 ± 9*	3.3 ± 0.5*	0.28 ± 0.08*
RES[HD]	358 ± 40*	33 ± 4*	24 ± 5*	86 ± 12*	3.8 ± 0.6*	0.25 ± 0.06*

[#]$P < 0.05$ vs. control group; *$P < 0.05$ vs. OVX group.

BMD, bone mineral density; BV/TV, bone volume/total volume; BS/BV, bone surface/bone volume; Tb. Th, trabecular thickness; Tb. N, trabecular number; Tb. Sp, trabecular separation.
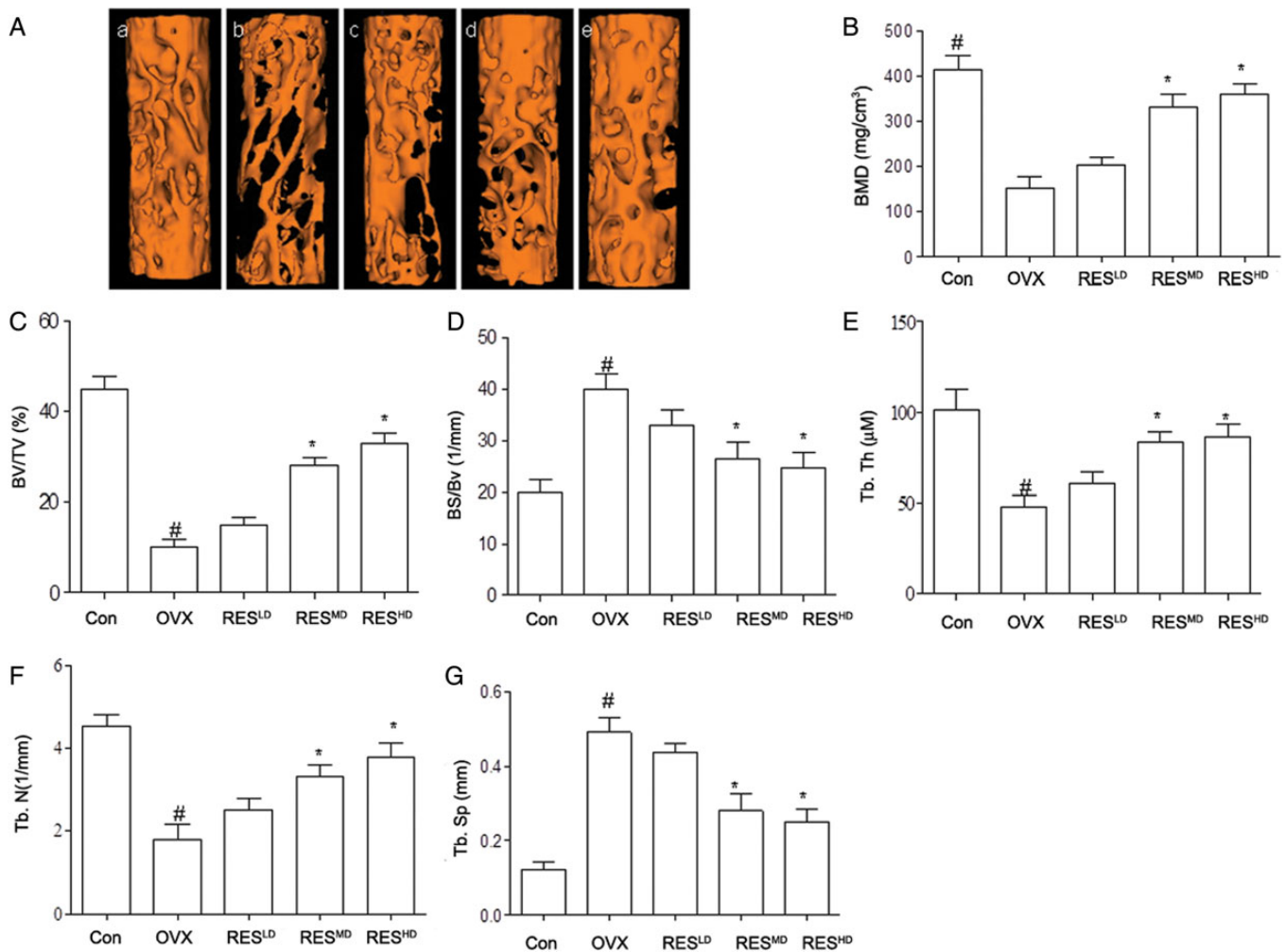
Figure 3. The change of parameters of micro-computed tomographic (CT) (A) Three dimensional reconstruction images of micro-CT. (a−e) Control group, ovariectomy (OVX) group, RES[LD] group, RES[MD] group, and RES[HD] group, respectively. (B−G) Resveratrol treatment improved parameters of micro-CT in OVX rats [(B) bone mineral density (BMD); (C) BV/TV; (D) BS/BV; (E) Tb. Th; (F) Tb. N; (G) Tb.Sp]. [#]$P < 0.05$ vs. control group; *$P < 0.05$ vs. OVX group. BV/TV, bone volume/total volume; BS/BV, bone surface/bone volume; Tb. Th, trabecular thickness; Tb. N, trabecular number; Tb. Sp, trabecular separation.

Postmenopausal osteoporosis is a common disease of the elderly women, characterized by low bone mass, microarchitectural deterioration and subsequent higher fracture occurrence [16,17]. World Health Organization defines osteoporosis as BMD is at least 2.5 standard deviations below the mean peak bone mass of young, healthy adults measured by DEXA [18].

OVX rat is a widely used model for the study of postmenopausal osteoporosis [19]. These alterations of bone are associated with estrogen deficiency, leading to imbalance
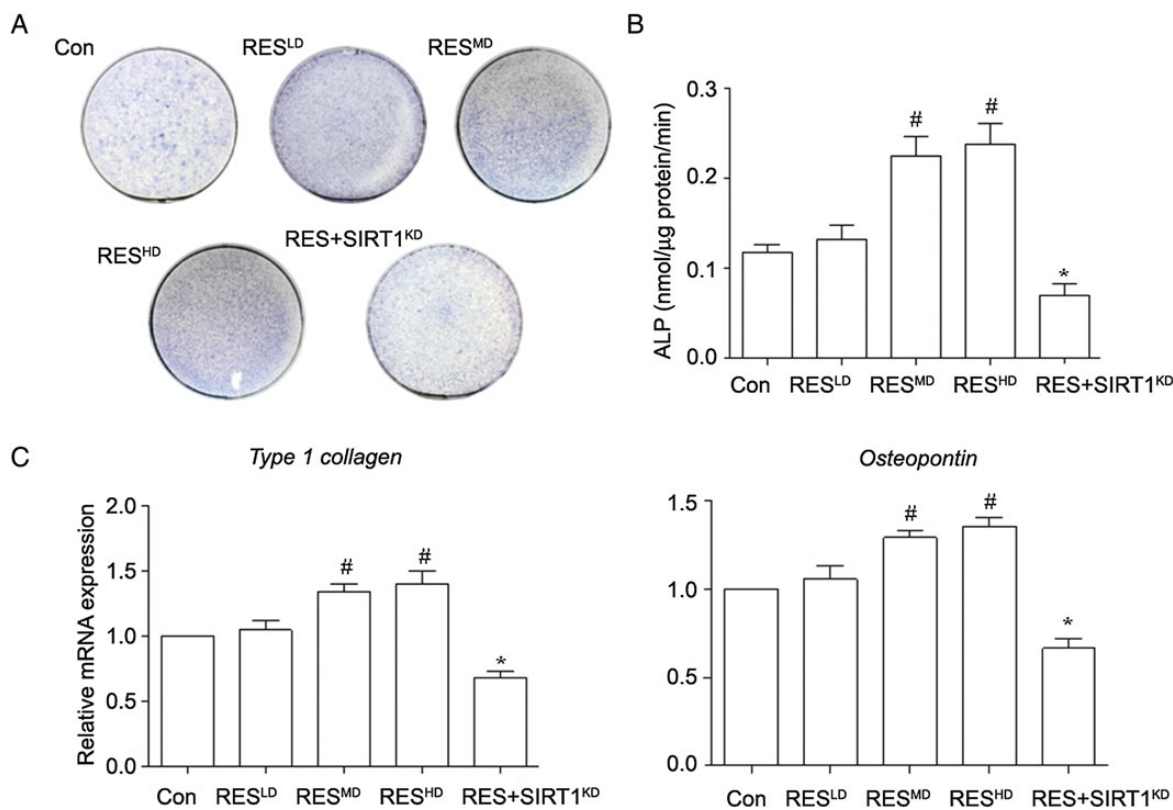
Figure 4. Resveratrol promoted osteoblast differentiation of BMSCs and this effect was blocked by siRNA-SIRT1 (A) Representative images of ALP staining of BMSCs on day 14. (B) Analysis of ALP activity. (C) Osteoblast specific genes (*type 1 collagen* and *osteopontin*) mRNA expression determined by real-time Polymerase chain reaction. [#]$P < 0.05$ vs. control group; *$P < 0.05$ vs. RES[HD] group. BMSCs, bone marrow mesenchymal stromal cells; ALP, alkaline phosphatase.
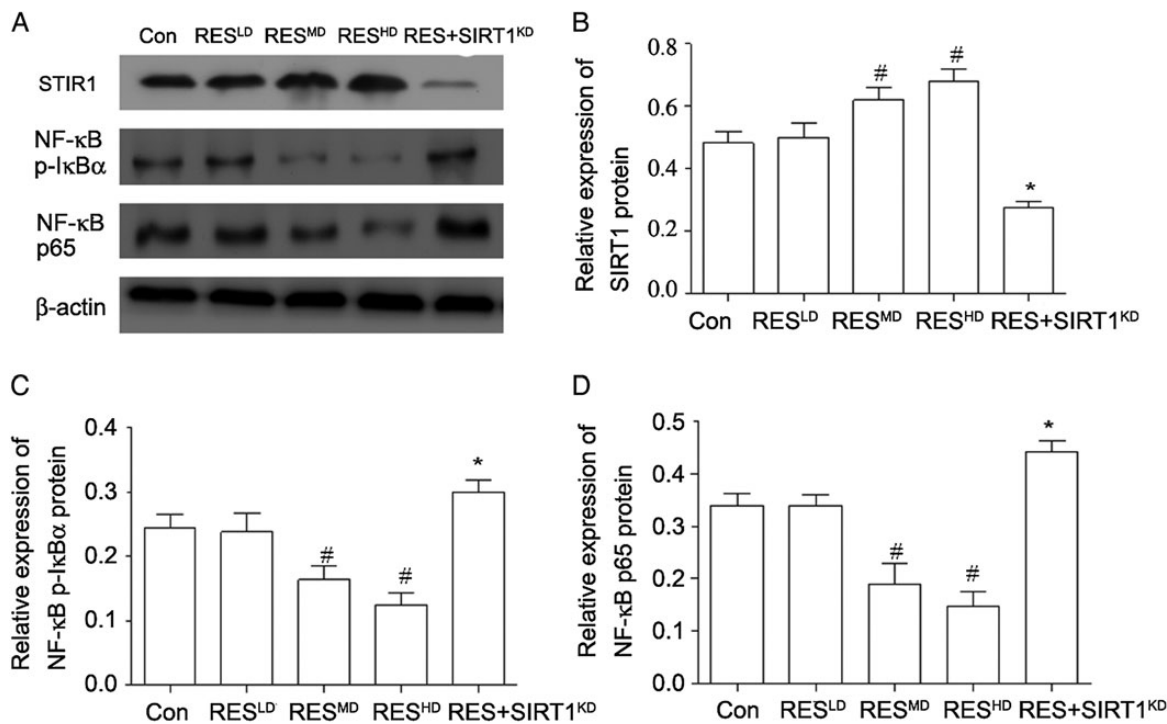
Figure 5. Resveratrol increased SIRT1 expression and suppressed NF-κB activity (A) Representative western blot bands of SIRT1, NF-κB proteins (p-IκBα and NF-κB p65) and β-actin. (B–D) Qualification analysis of SIRT1, NF-κB proteins (p-IκBα and NF-κB p65) expression (normalized to β-actin). [#]$P < 0.05$ vs. control group; *$P < 0.05$ vs. RES[HD] group.

between osteoblasts and osteoclasts. In this study, ovariectomy in rats was done to mimic osteoporosis status *in vivo*. A significant reduction of BMD in OVX rats was observed, suggesting a successful osteoporosis model. Microarchitectural deterioration is another important index for osteoporosis. The micro-CT and HE staining results both revealed that ovariectomy induced bone microarchitectural deterioration, characterized by thinning of bone trabeculae, increase of intertrabecular space and decease of BMD.

Several previous studies have reported the beneficial effects of resveratrol against OVX in rat models but the specific dose is uncertain. Mizutani *et al.* [20] reported that resveratrol at the dose of as low as 5 mg/kg/d was capable of preventing ovariectomy-induced decreases in bone strength. Controversially, in the study by Lin *et al.* [21], they applied resveratrol at the dose of 5, 15, and 45 mg/kg/d in OVX rats. Though BMD was increased in all of the three resveratrol treated groups, significant increase of BMD was only found in 45 mg/kg/d group. A limitation of their study was that they did not observe other parameters for osteoporosis except for BMD. Based on these previous studies, we applied three different doses of resveratrol: 5, 25, and 45 mg/kg/d and examined the therapeutic effects *in vivo*. There was a marked restoration of BMD in medium and high doses resveratrol treatment groups (25 and 45 mg/kg/d). In addition, medium and high doses of resveratrol treatment restored the damaged microarchitecture of OVX rat bone, evidenced by the improved bone trabeculae and intertrabecular space and fewer microfractures of bone trabeculae. But the low dose group (5 mg/kg/d) did not show significant changes. These findings were in accordance with our *in vitro* results. In our *in vitro* experiment, low concentration of resveratrol (20 μM) did not cause significant changes in ALP activity, type 1 collagen, and osteopontin expression. But 25 and 30 μM resveratrol led to statistically significant alterations. This could be explained by the fact that low dose of resveratrol (5 mg/kg/d or 20 μM) did not markedly elevate the expression of SIRT1 protein and subsequent NF-κB activities, as shown in western blot results. This indicated that the beneficial function of resveratrol was via the activation of SIRT1.

Another interesting finding in this study is the alterations of serum osteoporosis markers ALP and OC expression. ALP is an important enzyme in osteoid formation and mineralization. OC is a protein whose amount is in positive correlation with bone formation rates [20]. Both ALP and OC could be considered as marker proteins for bone turnover, presenting the relations between bone re-sorption, bone formation and bone mineralization. Increased ALP and OC could be observed in osteoporosis condition [21]. ALP is a serum marker for bone formation, and changes with the balance between osteoblast and osteoclast activity. As shown in our *in vivo* data, ALP level was elevated in OVX

rats but decreased in resveratrol treated group compared with OVX group, indicating the possibility that resveratrol prevent bone loss through decreased bone turnover. This could be explained because evidence has shown that resveratrol was capable of inhibiting osteoclast activity. Previous reports demonstrated that resveratrol inhibited osteoclast differentiation and decreased bone loss [12,13]. The inhibitory effect of resveratrol on osteoclast differentiation explained the decreased ALP level *in vivo* in resveratrol treated rats compared with OVX rats. The decreased serum ALP verified that resveratrol alleviated OVX induced osteoporosis *in vivo*. On the other hand, our *in vitro* data showed that resveratrol promoted osteoblast differentiation and increased bone formation, which was the reason why ALP was elevated in resveratrol treated cells *in vitro*. Our present results, combined with previous studies, demonstrated that resveratrol is capable of both promoting osteoblast differentiation and inhibiting osteoclastogenesis.

Interestingly, based on the structural similarity between resveratrol and estrogen, researchers hypothesized that resveratrol may serve as an estrogen receptor agonist. Zhao *et al.* [22] reported that long-term resveratrol treatment prevents ovariectomy-induced osteopenia in rats, but the underlying mechanism is still unclear. Thus, we further did *in vitro* study to explore the mechanisms of resveratrol treatment. It is known that estrogenic activity is associated with osteoporosis capacity and that bone formation function of osteoblasts is the primary beneficial cell type in osteoporosis. Considering this, we hypothesized that resveratrol was capable of promoting the amount and activity of osteoblasts, which contributed to the alleviation of osteoporosis after resveratrol treatment. To testify our hypothesis, we did *in vitro* study with BMSCs, which were potential for osteoblast differentiation. Resveratrol has been reported to play a positive role in osteoblast differentiation of BMSCs and adipose derived stromal cells [11,23]. Our study further verified that resveratrol could promote osteoblast differentiation of BMSCs. In our *in vitro* study, resveratrol treatment elevated ALP amount and activity. We further analyzed osteoblast-specific genes expression, such as t*ype I collagen* and *osteopontin*. The up-regulation of these genes further confirmed that resveratrol induced osteoblast differentiation of BMSCs.

The regulation of bone mineral formation and osteoblast differentiation is complex. We further explored the molecular mechanism by which resveratrol exert these beneficial effects. SIRT1 is a deacetylase involved in various physical and pathological processes, such as mitochondrial biogenesis and function, cell differentiation, aging, and inflammation [24]. Many molecules are regulated by SIRT1 via deacetylation effect, including NF-κB, AMPK, FoxO3a, and PGC-1α. Among them, NF-κB is a well-known molecule involved in various metastatic bone diseases [25]. It has been reported that NF-κB signaling pathway is an important

mediator in osteoblast differentiation [26,27]. Previous studies also reported that constitutive inhibition of NF-κB in Saos2 cells could increase the expression of osteoblast specific matrix protein collagen I and promote osteoblast differentiation [28,29]. Yeung *et al.* [30] found that SIRT1 protein directly interacted with Rel/p65 subunit of NF-κB and suppressed NF-κB transcriptional activity using resveratrol as an agonist in non-small-cell lung cancer cell line. However, no evidence has been shown for the molecular signaling of resveratrol against osteoblast differentiation. Based on these previous findings, we hypothesized that resveratrol-mediated SIRT1 activation inhibited the NF-κB signaling, thus promoted the osteoblast differentiation of BMSCs, which further accounted for the beneficial effects of resveratrol against osteoporosis *in vivo*. So we analyzed the expression of predominant molecules of NF-κB p-IκBα and NF-κB p65 by western blot analysis to reveal the activation of NF-κB in BMSCs. As expected, western blot results revealed that resveratrol activated SIRT1, and subsequently decreased the expression of NF-κB p-IκBα and NF-κB p65 in nuclear. Moreover, the beneficial effects of resveratrol, such as increase of osteoblast differentiation and inhibition of NF-κB activity, were blocked by siRNA-SIRT1 in RES+ SIRT1^{KD} group compared with RES^{HD} group, indicating that the effects of resveratrol were mediated by SIRT1. Previous studies reported that NF-κB was associated with osteoporosis as for its predominant role in osteoclastogenesis [31–33]. Here, our results demonstrated that NF-κB acts as a negative regulator in osteoblast differentiation, which also regulated the process of osteoporosis. Furthermore, we showed the evidence that resveratrol regulated SIRT1-NF-κB signaling pathway, promoted osteoblast differentiation, and protected against osteoporosis.

However, there is some limitation in this study. Osteoblasts and osteoclasts are both important cells involved in the occurrence of osteoporosis. In this *in vitro* study, we only detected the effects of resveratrol on osteoblasts. We did not investigate whether the inhibition of osteoclast was also associated in the beneficial effects of resveratrol. Further studies are still needed.

Taken together, our present study confirmed that resveratrol treatment could promote osteoblast differentiation of BMSCs *in vitro*, and alleviate the BMD reduction and microarchitectural deterioration induced by osteoporosis in ovariectomized rats. One important finding is that the beneficial effects of resveratrol against osteoporosis is dose dependent, and low dose of 5 mg/kg/d was insufficient whereas the dose of 25 and 45 mg/kg/d could cause significant alterations *in vivo*. Furthermore, our results verified that the protective role of resveratrol against osteoporosis was mediated by SIRT1-NF-κB signaling pathway. Our findings suggested the potential therapeutic role of resveratrol in osteoporosis treatment and stressed the importance of effective doses when applied.

Supplementary Data

Supplementary Data is available at *ABBS* online.

Acknowledgements

Funding

References

1. Silva I and Branco JC. Denosumab: recent update in postmenopausal osteoporosis. Acta Reumatol Port 2012, 37: 302–313.
2. Yilmaz M, Isaoglu U, Uslu T, Yildirim K, Seven B, Akcay F and Hacimuftuoglu A. Effect of methylprednisolone on bone mineral density in rats with ovariectomy-induced bone loss and suppressed endogenous adrenaline levels by metyrosine. Indian J Pharmacol 2013, 45: 344–347.
3. Noguchi Y, Kawate H, Nomura M and Takayanagi R. Eldecalcitol for the treatment of osteoporosis. Clin Interv Aging 2013, 8: 1313–1321.
4. Muir JM, Ye C, Bhandari M, Adachi JD and Thabane L. The effect of regular physical activity on bone mineral density in post-menopausal women aged 75 and over: a retrospective analysis from the Canadian multicentre osteoporosis study. BMC Musculoskelet Disord 2013, 14: 253.
5. Raisz LG. Pathogenesis of osteoporosis: concepts, conflicts, and prospects. J Clin Invest 2005, 115: 3318–3325.
6. Rossouw JE, Anderson GL, Prentice RL, LaCroix AZ, Kooperberg C, Stefanick ML and Jackson RD, *et al*. Risks and benefits of estrogen plus progestin in healthy postmenopausal women: principal results from the Women's Health Initiative randomized controlled trial. JAMA 2002, 288: 321–333.
7. Morris BJ. Seven sirtuins for seven deadly diseases of aging. Free Radic Biol Med 2013, 56: 133–171.
8. Yao H and Rahman I. Perspectives on translational and therapeutic aspects of SIRT1 in inflammaging and senescence. Biochem Pharmacol 2012, 84: 1332–1339.
9. Rahman I, Kinnula VL, Gorbunova V and Yao H. SIRT1 as a therapeutic target in inflammaging of the pulmonary disease. Prev Med 2012, 54: S20–S28.
10. Guerrero RF, Garcia-Parrilla MC, Puertas B and Cantos-Villar E. Wine, resveratrol and health: a review. Nat Prod Commun 2009, 4: 635–658.
11. Mobasheri A and Shakibaei M. Osteogenic effects of resveratrol *in vitro*: potential for the prevention and treatment of osteoporosis. Ann N Y Acad Sci 2013, 1290: 59–66.
12. He X, Andersson G, Lindgren U and Li Y. Resveratrol prevents RANKL-induced osteoclast differentiation of murine osteoclast progenitor RAW 264.7 cells through inhibition of ROS production. Biochem Biophys Res Commun 2010, 401: 356–362.
13. Shakibaei M, Buhrmann C and Mobasheri A. Resveratrol-mediated SIRT-1 interactions with p300 modulate receptor activator of NF-kappaB ligand (RANKL) activation of NF-kappaB signaling and inhibit osteoclastogenesis in bone-derived cells. J Biol Chem 2011, 286: 11492–11505.
14. Hou J, Chong ZZ, Shang YC and Maiese K. Early apoptotic vascular signaling is determined by Sirt1 through nuclear shuttling, forkhead

trafficking, bad, and mitochondrial caspase activation. Curr Neurovasc Res 2010, 7: 95–112.

15. Alles N, Soysa NS, Hayashi J, Khan M, Shimoda A, Shimokawa H and Ritzeler O, *et al*. Suppression of NF-kappaB increases bone formation and ameliorates osteopenia in ovariectomized mice. Endocrinology 2010, 151: 4626–4634.

16. French L, Smith M and Shimp L. Prevention and treatment of osteoporosis in postmenopausal women. J Fam Pract 2002, 51: 875–882.

17. Selby P. Postmenopausal osteoporosis. Curr Osteoporos Rep 2004, 2: 101–106.

18. Kanis JA. Assessment of fracture risk and its application to screening for postmenopausal osteoporosis: synopsis of a WHO report. WHO Study Group. Osteoporos Int 1994, 4: 368–381.

19. Cho P, Schneider GB, Krizan K and Keller JC. Examination of the bone-implant interface in experimentally induced osteoporotic bone. Implant Dent 2004, 13: 79–87.

20. Mizutani K, Ikeda K, Kawai Y and Yamori Y. Resveratrol attenuates ovari-ectomy-induced hypertension and bone loss in stroke-prone spontaneously hypertensive rats. J Nutr Sci Vitaminol (Tokyo) 2000, 46: 78–83.

21. Lin Q, Huang YM, Xiao BX and Ren GF. Effects of resveratrol on bone mineral density in ovarectomized rats. Int J Biomed Sci 2005, 1: 76–81.

22. Zhao H, Li X, Li N, Liu T, Liu J, Li Z and Xiao H, *et al*. Long-term resvera-trol treatment prevents ovariectomy-induced osteopenia in rats without hyperplastic effects on the uterus. Br J Nutr 2014, 111: 836–846.

23. Dosier CR, Erdman CP, Park JH, Schwartz Z, Boyan BD and Guldberg RE. Resveratrol effect on osteogenic differentiation of rat and human adipose derived stem cells in a 3-D culture environment. J Mech Behav Biomed Mater 2012, 11: 112–122.

24. Kitada M and Koya D. SIRT1 in Type 2 diabetes: mechanisms and thera-peutic potential. Diabetes Metab J 2013, 37: 315–325.

25. Vassiliou V. Management of metastatic bone disease in the elderly with bisphosphonates and receptor activator of NF-κB ligand inhibitors: effect-iveness and safety. Clin Oncol (R Coll Radiol) 2013, 25: 290–297.

26. Yao Z, Li Y, Yin X, Dong Y, Xing L and Boyce BF. NF-kappaB RelB negatively regulates osteoblast differentiation and bone formation. J Bone Miner Res 2014, 29: 866–877.

27. Feng X, Feng G, Xing J, Shen B, Li L, Tan W and Xu Y, *et al*. TNF-alpha triggers osteogenic differentiation of human dental pulp stem cells via the NF-kappaB signalling pathway. Cell Biol Int 2013, 37: 1267–1275.

28. Eliseev RA, Schwarz EM, Zuscik MJ, O'Keefe RJ, Drissi H and Rosier RN. Smad7 mediates inhibition of Saos2 osteosarcoma cell differentiation by NF-kappaB. Exp Cell Res 2006, 312: 40–50.

29. Andela VB, Sheu TJ, Puzas EJ, Schwarz EM, O'Keefe RJ and Rosier RN. Malignant reversion of a human osteosarcoma cell line, Saos-2, by inhib-ition of NFkappaB. Biochem Biophys Res Commun 2002, 297: 237–241.

30. Yeung F, Hoberg JE, Ramsey CS, Keller MD, Jones DR, Frye RA and Mayo MW. Modulation of NF-kappaB-dependent transcription and cell sur-vival by the SIRT1 deacetylase. EMBO J 2004, 23: 2369–2380.

31. Hsiao HB, Lin H, Wu JB and Lin WC. Kinsenoside prevents ovariectomy-induced bone loss and suppresses osteoclastogenesis by regulating classical NF-kappaB pathways. Osteoporos Int 2013, 24: 1663–1676.

32. Liou SF, Hsu JH, Lin IL, Ho ML, Hsu PC, Chen LW and Chen IJ, *et al*. KMUP-1 suppresses RANKL-induced osteoclastogenesis and prevents ovariectomy-induced bone loss: roles of MAPKs, Akt, NF-kappaB and calcium/calcineurin/NFATc1 pathways. PLoS One 2013, 8: e69468.

33. Li DZ, Zhang QX, Dong XX, Li HD and Ma X. Treatment with hydrogen molecules prevents RANKL-induced osteoclast differentiation associated with inhibition of ROS formation and inactivation of MAPK, AKT and NF-kappa B pathways in murine RAW264.7 cells. J Bone Miner Metab 2014, 32: 494–504.